FILE COPY

NWC TP 6890

(4)

Evaluation of Forest Fire Burn Model of Reaction Kinetics of Heterogeneous Explosives

by
E. A. Lundstrom
Research Department

MAY 1988

AD-A200 411

NAVAL WEAPONS CENTER
CHINA LAKE, CA 93555-6001

Approved for public release; distribution is unlimited

DTIC
ELECTE
JUL 18 1988
S D
H

88 7 18 006

Naval Weapons Center

FOREWORD

This report summarizes certain results obtained during investigation of high-speed fragment impact onto cased munitions. The Forest Fire burn model for energetic heterogeneous materials is investigated, modifications are developed, and the result is compared with experiment.

The work was performed during fiscal year 1967 at the Naval Weapons Center, China Lake, Calif., under funding from the Insensitive Munitions Advanced Development Program, Program Element 63609. Advanced development support of theoretical, experimental, and analytical work related to reactive behavior of explosives and propellants is essential to development of a solid technology base for the design of insensitive munitions.

This report was reviewed for technical accuracy by C. D. Lind.

Approved by
R. L. DERR, *Head*
Research Department
15 April 1968

Under authority of
J. A. BURT
Capt., U.S. Navy
Commander

Released for publication by
G. R. SCHIEFER
Technical Director

NWC Technical Publication 5898

Published by ..... Technical Information Department
Collation ..... 14 leaves
First Printing ..... 215 copies

UNCLASSIFIED

SECURITY CLASSIFICATION OF THIS PAGE (*When Data Entered*)

AD-A202411

REPORT DOCUMENTATION PAGE

1a. REPORT SECURITY CLASSIFICATION UNCLASSIFIED	1b. RESTRICTIVE MARKINGS
2a. SECURITY CLASSIFICATION AUTHORITY	3. DISTRIBUTION/AVAILABILITY OF REPORT Approved for public release; distribution is unlimited.
2b. DECLASSIFICATION/DOWNGRADING SCHEDULE	
4. PERFORMING ORGANIZATION REPORT NUMBER(S) NWC TP 6898	5. MONITORING ORGANIZATION REPORT NUMBER(S)
6a. NAME OF PERFORMING ORGANIZATION Naval Weapons Center 6b. OFFICE SYMBOL (If Applicable)	7a. NAME OF MONITORING ORGANIZATION
6c. ADDRESS (*City, State, and ZIP Code*) China Lake, CA 93555-6001	7b. ADDRESS (*City, State, and ZIP Code*)
8a. NAME OF FUNDING/SPONSORING ORGANIZATION 8b. OFFICE SYMBOL (If Applicable)	9. PROCUREMENT INSTRUMENT IDENTIFICATION NUMBER
8c. ADDRESS (*City, State, and ZIP Code*)	10. SOURCE OF FUNDING NUMBERS PROGRAM NO. 63609N; PROJECT NO. 3131 24; TASK NO. S0 363; WORK UNIT 132080

11. TITLE (*Include Security Classification*)

EVALUATION OF FOREST FIRE BURN MODEL OF REACTION KINETICS OF HETEROGENEOUS EXPLOSIVES (U)

12. PERSONAL AUTHOR(S)

Lundstrom, Eric A.

13a. TYPE OF REPORT	13b. TIME COVERED	14. DATE OF REPORT (Year, Month, Day)	15. PAGE COUNT
Summary	From 1987 To 1988	1988, May	23

16. SUPPLEMENTARY NOTATION

17. COSATI CODES			18. SUBJECT TERMS (*Continue on reverse side if necessary and identify by block number*)
FIELD	GROUP	SUB-GROUP	

19. ABSTRACT (*Continue on reverse side if necessary and identify by block number*)

(U) Forest Fire is a global reaction kinetics model for the high-pressure chemical decomposition of heterogeneous explosives. The model, named for its originator, C. Forest, is calibrated with the results of wedge tests. The calibration technique is based on an analysis of the shock-to-detonation process observed in the wedge test, and incorporates several assumptions regarding the shock acceleration process and the order of the decomposition kinetics. These assumptions are examined here in terms of their validity in the wedge test process and their consequences in the resulting reaction model. It is found that a special case of Forest's analysis is a better description of the wedge test process, and, when combined with simplified kinetics, good reaction rate estimates are obtained. In addition, the modified calibration method can be used to estimate the reaction rates in the (contd. on back page)

20. DISTRIBUTION/AVAILABILITY OF ABSTRACT	21. ASTRACT SECURITY CLASSIFICATION	
☒ UNCLASSIFIED/UNLIMITED ☐ SAME AS RPT. ☒ DTIC USERS	Unclassified	
22a. NAME OF RESPONSIBLE INDIVIDUAL Eric A. Lundstrom	22b. TELEPHONE (*Include Area Code*) (619) 939-2206	22c. OFFICE SYMBOL Code 3894

DD FORM 1473, 84 MAR

83 APR edition may be used until exhausted.
All other editions are obsolete.

SECURITY CLASSIFICATION OF THIS PAGE
UNCLASSIFIED

19. (Contd.)
high-pressure detonation regime where the conventional analysis fails.

CONTENTS

DTIC COPY INSPECTED

Accession For
NTIS GRA&I
DTIC TAB
Unannounced
Justification
By
Distribution/
Availability Codes
Dist | Avail and/or special
A-1

INTRODUCTION

One of the central goals in explosives science is to extrapolate the results of simple small-scale testing to predict the outcome of complex problems of practical interest. A remarkable procedure has been developed by C. Forest (Reference 1) that has enabled engineering calculations for a variety of problems involving shock-initiated reaction of heterogeneous solid explosives. Forest assumed a global reaction rate model for the decomposition of the explosive and derived a method to calibrate the model using the results of wedge tests. The result is popularly known as the "Forest Fire" burn-rate model. The reaction model is then used in one- and two-dimensional hydrodynamics computer codes where the details of shock wave interactions with reacting explosive materials can be calculated. This procedure has been successfully applied to a variety of very practical problems. (See References 2, 3, and 4, for examples.)

In the selection of the reaction model and the derivation of its calibration procedure, Forest makes an assumption about the processes that occur in the explosive decomposition that is contrary to the widely held view of hot spot initiation of heterogeneous explosives. He also makes several assumptions about the flow field obtained in the wedge test that affect the calibration of the reaction model. These assumptions are inconsistent with calculations using the burn model. That is, when the Forest Fire burn model is used to calculate wedge test results, one does not obtain the flow field assumed in the calibration of the model.

In spite of inconsistencies in the theory, one is faced with a rather impressive history of success in correlating experiment with calculation for a wide variety of applications. Therefore, an attempt is made here to evaluate the effect of the various assumptions of the Forest Fire theory. The method used is to evaluate the reaction rates based on extreme cases of the assumptions and to evaluate their effect on results of numerical calculations of the wedge test.

FLOW FIELD ANALYSIS

As a model of the shock-to-detonation transition observed in the wedge test, Forest proposed a hydrodynamic discontinuity within which some fraction of the solid reactants is converted (burned) to gaseous products. In one extreme case, no solid is burned and the discontinuity is the familiar shock wave. In the other extreme, all of the solid is consumed and one has a detonation wave. In the following, the hydrodynamic discontinuity will also be called a reacting shock wave. A wave diagram of an accelerating shock wave is shown in Figure 1. At a distance X_d the wave transitions to Chapman-Jouguet (CJ) detonation and the wave velocity is constant thereafter. The transition to detonation may be smooth or it may be

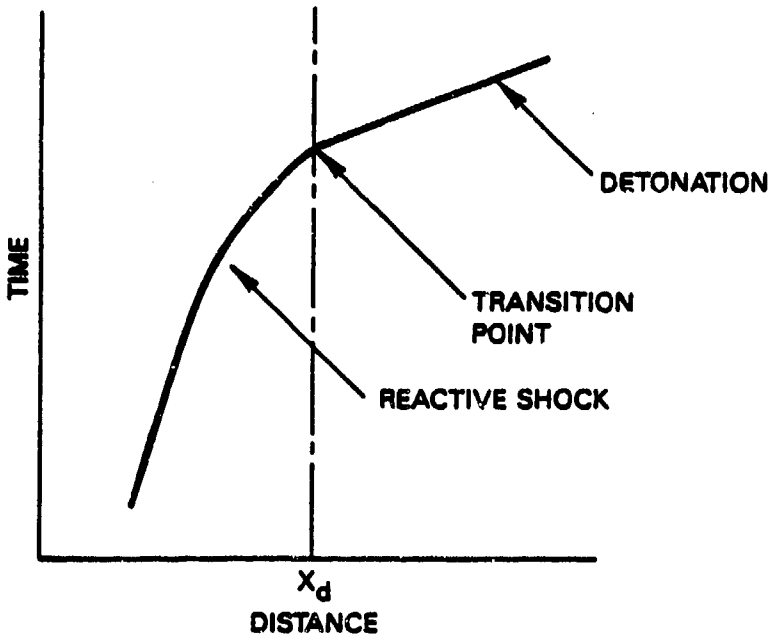

FIGURE 1. Time-Space Diagram of Runup of a Reactive Shock Wave to a Detonation.

discontinuous. The fraction of solid burned within the reacting shock wave increases with wave propagation distance (or time) until it is all burned at X_d. In addition to combustion, which occurs instantaneously within the discontinuity, the remaining solid continues to burn behind the wave at some finite rate. The objective of the flow field analysis is to calculate the burn rate behind the wave as a function of pressure and the velocity of the wave.

To calculate the burn rate, one starts with the Lagrangian equations for conservation of mass, momentum, and energy (Reference 2)

$$U_t = -P_m \tag{1a}$$

$$V_t = U_m \tag{1b}$$

$$E_t = -PV_t \tag{1c}$$

and an arbitrary equation of state

$$P = P(V,E,W) \tag{1d}$$

where V, U, E, P, and W are the specific volume, velocity, energy per unit initial volume, pressure, and solid mass fraction, respectively. The subscripts t and m denote partial derivatives with respect to time and the Lagrangian mass coordinate. In addition, one has the

jump equations expressing conservation of mass, momentum, and energy across the reacting shock wave (Reference 2)

$$P_1 = U_s U_1 / V_0 \tag{2a}$$

$$V_1 U_s = V_0 (U_s - U_1) \tag{2b}$$

$$E_1 = U_1^2/2 \tag{2c}$$

and the equation of state

$$P_1 = P(V_1, E_1, W_1) \tag{2d}$$

where the subscripts 0 and 1 denote conditions in the uniform initial state and the state just downstream of the reactive shock wave. The velocity of the reactive shock is given by U_s. Equation 2 assumed that $P_0 = 0$, $E_0 = 0$, and $U_0 = 0$. Note that since the material is allowed to partially react within the discontinuity, there are six variables and four equations, leaving two degrees of freedom instead of the usual one.

Forest calculated the burn rate W_τ as a function of thermodynamic parameters at state 1, the pressure gradient P_m, and what amounts to the wave acceleration. He found that a zero pressure gradient P_m gave good results. For simplicity, the pressure gradient is allowed to vanish here early in the derivation.

The burn rate, W_τ, can be obtained by differentiating the equation of state (Equation 1d)

$$P_\tau = P_V V_\tau + P_E E_\tau + P_W W_\tau \tag{3}$$

where the derivatives

$$P_V = \left(\frac{\partial P}{\partial V}\right)_{E,W}$$

$$P_E = \left(\frac{\partial P}{\partial E}\right)_{V,W}$$

$$P_W = \left(\frac{\partial P}{\partial W}\right)_{E,V}$$

are known functions of V, E, and W and are computed numerically from Equation 2d. The time derivatives V_τ and E_τ are next eliminated from Equation 3 in favor of the velocity gradient, U_m, using Equation 1, yielding

$$P_\tau = (P_V - P P_E) U_m + P_W W_\tau \tag{4}$$

It is desired to express the derivatives P_τ and U_m in favor of the pressure gradient P_m and derivatives in the direction of shock propagation, since these are known at the shock boundary.

To obtain directional derivatives, a simple exercise of the chain rule gives

$$\left(\frac{\partial P}{\partial \tau}\right)_s = P_\tau + P_m \left(\frac{\partial m}{\partial \tau}\right)_s \tag{5}$$

and

$$\left(\frac{\partial U}{\partial \tau}\right)_s = U_\tau + U_m \left(\frac{\partial m}{\partial \tau}\right)_s \tag{6}$$

where the notation $(\partial/\partial\tau)_s$ denotes a time derivative in a direction on the space-time plane that is parallel to the direction of the travel of the reactive shock. Using Equation 1b for U_τ, while noting that $(\partial m/\partial\tau)_s = U_s/V_0$, and evaluating the result at the shock boundary, Equations 5 and 6 yield

$$P_\tau = \frac{dP_1}{d\tau_1} - P_m U_s \Big/ V_0 \tag{7}$$

and

$$U_m = \left(\frac{dU_1}{d\tau_1} + P_m\right) V_0 \Big/ U_s \tag{8}$$

Here it is convenient to impose the simplifying assumption $P_m = 0$. Substituting Equations 7 and 8 into 4, one obtains

$$W_\tau = \left[\frac{dP_1}{d\tau_1} - \left(P_V - P_1 P_E\right) \frac{dU_1}{d\tau_1} \frac{V_0}{U_s}\right] \Big/ P_W \tag{9}$$

Instead of derivatives with respect to τ_1, the shock position, x_1, is a more convenient variable and so Equation 9 becomes

$$W_\tau = \left[U_s \frac{dP_1}{dx_1} - \left(P_V - P_1 P_E\right) V_0 \frac{dU_1}{dx_1}\right] \Big/ P_W \tag{10}$$

Equation 10 is a preliminary result obtained by Forest in Reference 5.

In order to relate the two derivatives, dU_1/dx_1 and dP_1/dx_1, the reaction that takes place within the discontinuity must be specified. Forest proposes a "reactive" Hugoniot in the form of

$$U_s = C_r + S_r U_1 \tag{11}$$

This equation, together with Equation 2, determines W_1 at the shock boundary. Combining Equation 11 with Equation 2a to eliminate the shock velocity, U_s, and differentiating the result, one gets

$$V_0 \frac{dP_1}{dx_1} = \left(C_r + 2S_r U_1\right) \frac{dU_1}{dx_1} \tag{12}$$

Substituting Equation 12 into Equation 10, one gets

$$W_r = \left[U_s - V_0^2 \frac{P_V - P_1 P_E}{C_r + 2S_r U_1}\right] \frac{1}{P_W} \frac{dP_1}{dx_1} \tag{13}$$

relating the reaction rate W_r to the rate of pressure increase at the shock front.

An alternate and more self-consistent assumption is a nonreactive shock front with $W_1 = 1$. For some equations of state, the nonreactive Hugoniot reduces to the form of Equation 11 with particular choices of C_r and S_r. This is true with the HOM equation of state (Reference 2) used by Forest. In this case, Equation 13 can be applied to the nonreactive shock case by proper choice of C_r and S_r. For other equations of state, one can derive a relation equivalent to Equation 12 as follows. First differentiate Equation 2d with W_1 constant and eliminate the derivative dE_1/dx_1 with Equation 2c to obtain

$$\frac{dP_1}{dx_1} = P_V \frac{dV_1}{dx_1} + 2P_E U_1 \frac{dU_1}{dx_1} \tag{14}$$

Then combine Equations 2a and 2b to eliminate U_s and differentiate the result to get

$$\left(V_0 - V_1\right)\frac{dP_1}{dx_1} - P_1 \frac{dV_1}{dx_1} = 2U_1 \frac{dU_1}{dx_1} \tag{15}$$

Eliminate dV_1/dx_1 between Equations 15 and 14 and solve for $\dfrac{dU_1}{dx_1}$ to obtain the result

$$\frac{dU_1}{dx_1} = \frac{P_1 - (V_0 - V_1)P_V}{2U_1(P_1 P_E - P_V)} \frac{dP_1}{dx_1} \tag{16}$$

Substituting Equation 16 into Equation 10 to eliminate dU_1/dx_1 and simplifying the result with Equation 2b gives

$$W_t = \left[\frac{3P_1 - (V_0 - V_1)P_V}{2U_1} \right] \frac{V_0}{P_W} \frac{dP_1}{dx_1} \tag{17}$$

which is equivalent to Equation 13 for a nonreactive shock but is valid for any equation of state.

Given the pressure rate of increase with distance, dP_1/dx_1, then Equation 13 or 17 may be employed to calculate the required reaction rate (provided that $P_m = 0$ is valid). When one performs an experiment where W_1 and the thermodynamic state is known, then, in effect, one measures the reaction rate as a function of that thermodynamic state. Forest uses the wedge test for this purpose.

In the wedge test, a shock wave is introduced into an explosive where it accelerates to become a detonation wave within a length called the run distance. A plot of the run distance as a function of pressure is called a Pop plot after its originator, A. Popolato. When the logarithm of the run distance is plotted against the logarithm of the initial shock pressure, a straight line is often obtained over a large range of pressure. These data have been obtained for a wide variety of explosives and detonable propellants. For the wedge test—experiments with initial shocks having different initial pressure—the "single-curve buildup principle" is observed to be a good approximation. (See Reference 6 for a good discussion of this.) This principle postulates that the shock that accelerates to detonation passes through a unique space-time trajectory regardless of the initial shock pressure. Accordingly, the Pop plot, taken from the results of several experiments, is also the pressure-distance history for any single test. For a Pop plot correlation in the form of

$$\ell n\, X_r = A + B\, \ell n\, P \tag{18}$$

where A and B are constants, X_r is the run distance, and P is the initial pressure, the single-curve buildup principle yields

$$\frac{dP_1}{dx_1} = -\frac{dP_1}{dX_r} = -\frac{P_1}{BX_r} \tag{19}$$

Substituting Equation 19 into Equation 13 or Equation 17, one gets an explicit expression for the reaction rate W_t as a function of the thermodynamic state of the material.

REACTION KINETICS

Forest assumes that the reaction of the explosive takes place according to a simple first-order decomposition reaction. Therefore, he fits the reaction rates calculated above to the following expression for first-order kinetics:

$$W_t/W = f(P) \tag{20}$$

where the reaction rate constant $f(P)$ is independent of the solid mass fraction and is expressed solely as a function of pressure. The choice of pressure as the independent variable for the reaction rate constant is not unique; temperature, or internal energy, or any other combination of state variables (such as in the HYDROX computer code in Reference 7) could have been just as easily chosen.

The first-order kinetics formula is based on the law of mass action and is useful as a global model of unimolecular decomposition reactions (Reference 8). It is not clear that this is the dominating reaction mechanism in the shock-initiated combustion of heterogeneous explosives. There is a problem with calibrating Equation 20 at high pressures, where W_t is finite and well-behaved while W_1 can become small or vanish, depending upon the choice of the reacting shock Hugoniot. In some of the numerical hydrodynamics codes that utilize Forest Fire, the rate is set to infinity whenever the pressure becomes greater than the CJ value. This is accomplished numerically simply by converting all remaining solid explosive to gaseous products when the CJ pressure is exceeded. This feature makes application of Forest Fire difficult for problems where the reaction zone of the detonation wave must be resolved.

An alternate hypothesis to the first-order kinetics assumption used by Forest is the ignition and growth concept used to describe explosive decomposition by Lee and Tarver (Reference 9), and Tarver and Hallquist (Reference 10). The shock initiation of the heterogeneous solid explosive is modeled by ignition at localized hot spots, followed by grain burning at the growing boundaries. This model has had some success in correlating the detailed mass velocity profiles in the flow field behind the shock during shock-to-detonation experiments, lending credibility to the basic concept. According to the ignition and growth model, the global reaction rate is a minimum at the shock boundary where $W_1 = 1$ because of the small burn-surface area of the hot spots. This is in direct opposition to the assumption of first-order kinetics, where the reaction is maximum at the shock.

For comparison with the first-order kinetics assumption, an alternate global model for the explosive decomposition is

$$W_t = f(P) \tag{21}$$

which ignores all dependence of the reaction rate on the solid mass fraction. In the following calculations, Equation 21 will be referred to as the constant rate model. This model should lie somewhere between the extremes of the ignition and growth burn model and the first-order kinetics employed by Forest. It can be noted that Equation 21 does not have the singularity when $W_1 = 0$, as Equation 20 does.

NUMERICAL CALCULATIONS

The effect of the various assumptions employed in the Forest Fire burn model derivation are best tested numerically. The calculations will employ the explosive PBX-9404 because of the large amount of experimental data available for it. The equations and constants for the HOM equation of state for PBX-9404 are given in Reference 2. These are used except for the Hugoniot of the unreacted explosive and the wedge test run distance correlation (Pop plot), which are obtained from Reference 11.

Partially reacting Hugoniot curves with constant W_1 are calculated for 9404 and are plotted on the P-V plane in Figure 2. The unreacting shock Hugoniot is the curve labeled $W_1 = 1$ in the figure, and the CJ point for steady detonation is labeled on the combustion products ($W_1 = 0$) curve. Reacting Hugoniot curves corresponding to different choices of the constants C_r and S_r in Equation 11 can also be represented on the P-V plane. For one choice of the constants, the reacting Hugoniot passes through both the initial state and the CJ point. This Hugoniot is shown on Figure 2 and will be used for the reacting shock example in the following calculations. The explosive solid fraction W_1 is not constant on this curve. The variation of solid fraction with pressure along the reacting shock Hugoniot is shown in Figure 3. The unreacting shock Hugoniot that will be used for comparison in the calculations is the $W_1 = 1$ curve in Figure 2.

The reaction rate, W_2, was calculated using Equation 13 for both reacting and unreacting shock hypotheses, and the result plotted in Figure 4. At low pressures, the results are nearly identical. It is only at pressures near the CJ point that the reactive shock case gives slightly higher reaction rates. The difference between the two curves is negligible compared to differences induced by the choice of the reaction model.

In Figure 5, the quotient W_2/W_1 is plotted as a function of pressure for both the reacting shock case and the nonreacting case, where for the latter $W_1 = 1$. The difference between the two results is substantial, particularly at high pressures where, according to Figure 3, W_1 goes to zero as the CJ pressure is approached. Physically, very little reaction takes place within the shock, and the numerical codes where the Forest Fire burn model is employed do not include such a phenomenon. Therefore, the assumption of a reacting shock wave used by Forest to calculate the reaction rates is not satisfied in the resulting numerical calculations. The further assumption of first-order kinetics exaggerates the consequences of the reactive shock assumption.

To compare the effect of the various assumptions and models, calculations are made of the run distance obtained in the wedge test. A one-dimensional Lagrangian hydrodynamics computer code was used for the calculations. It uses the SIN code algorithm described in Reference 2.

There is some arbitrariness in a general simulation of the wedge test because of the different types of shock attenuators and explosive drivers actually used in the tests. These are necessary in order to introduce shock waves of different intensities into the explosive

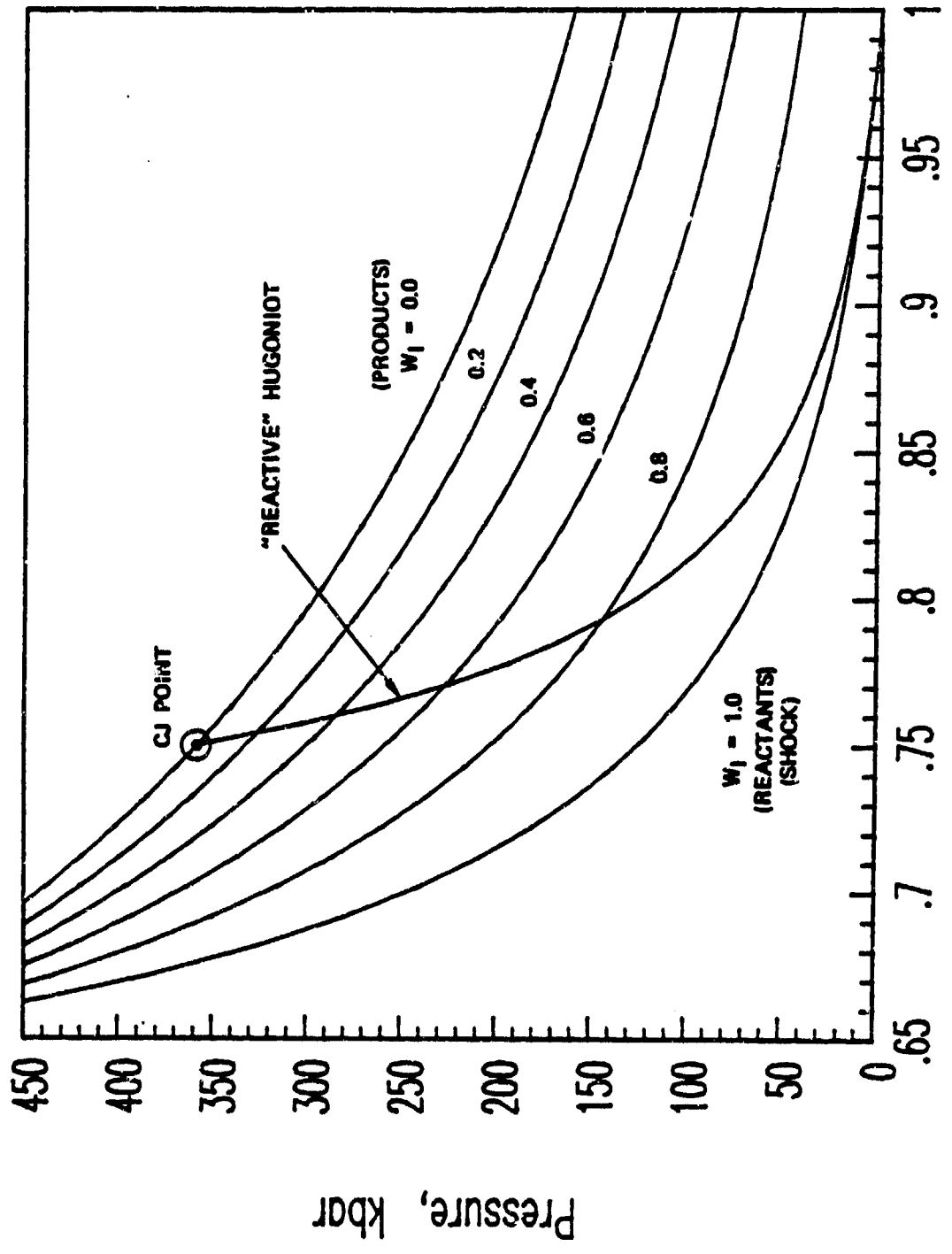

FIGURE 2. Partially Reacting (W_1 = Constant) Hugoniot Curves for PBX-9404. The reactive shock Hugoniot that passes through the initial and CJ states is shown.

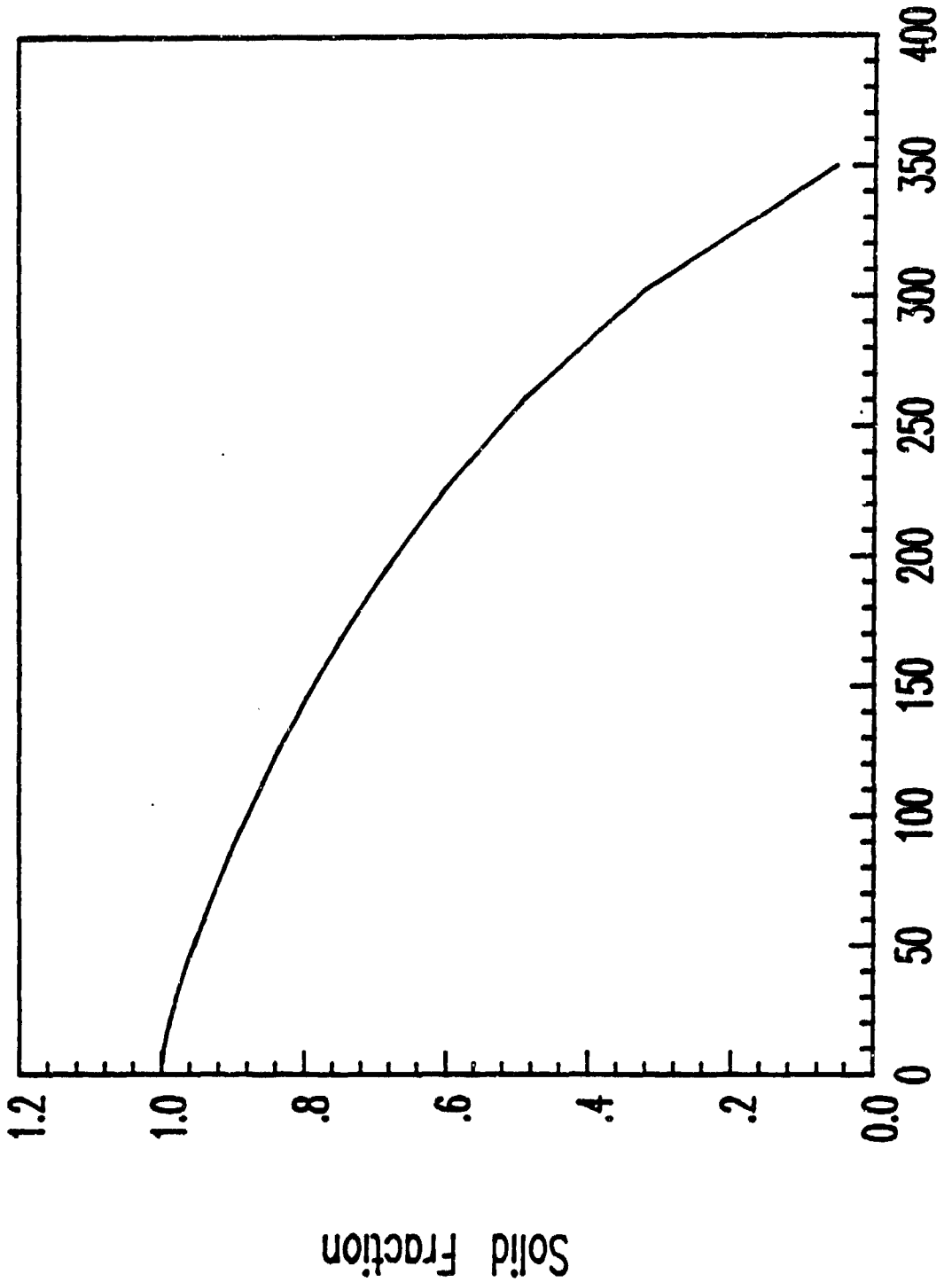

FIGURE 3. Solid Fraction as a Functioning of Shock Pressure for Reactive Hugoniot Plotted in Figure 2.

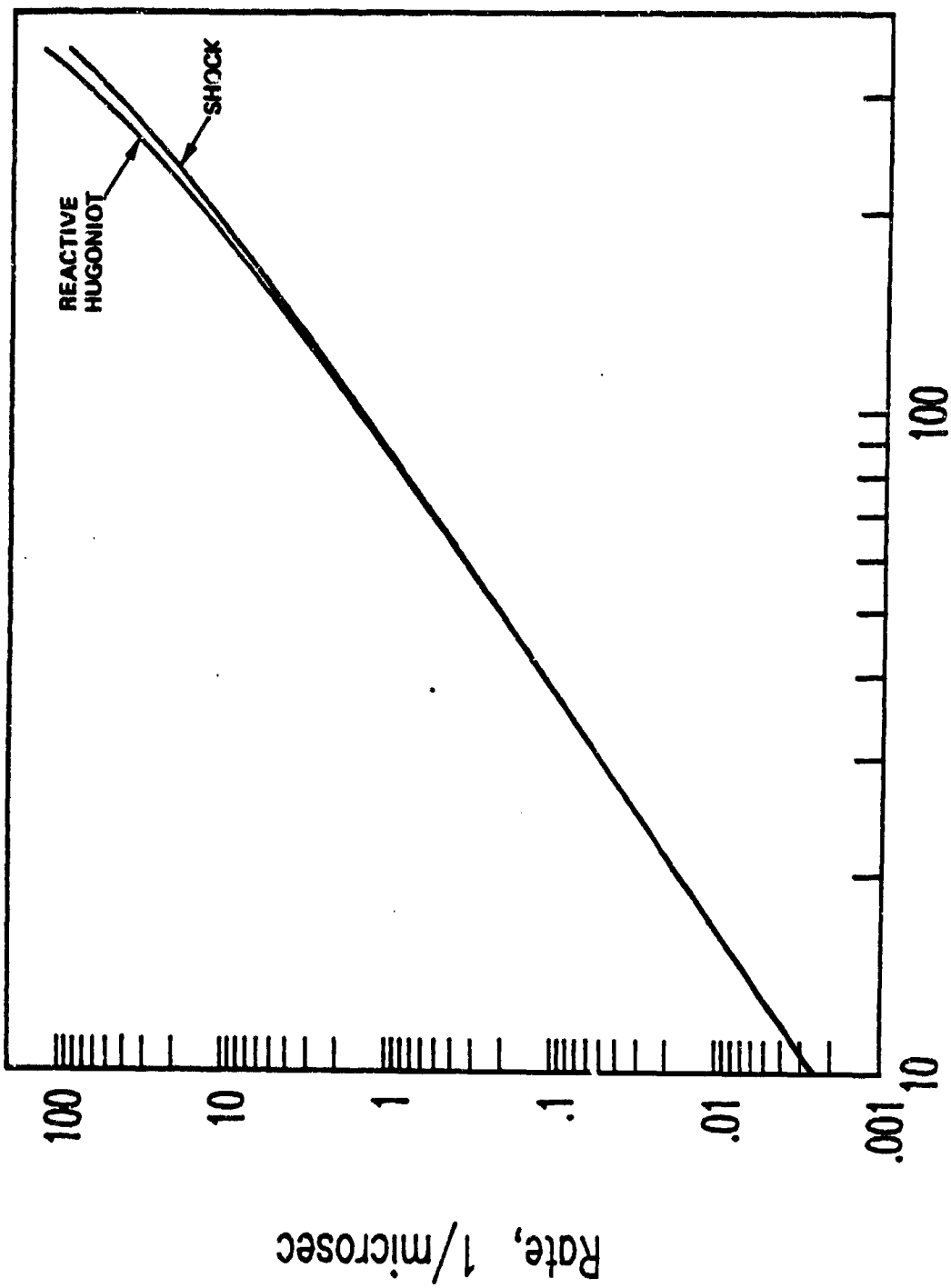

FIGURE 4. Reaction Rate – W_1 Plotted as Function of Pressure Comparing Results Obtained With Reactive Hugoniot and Nonreactive Shock Assumptions.

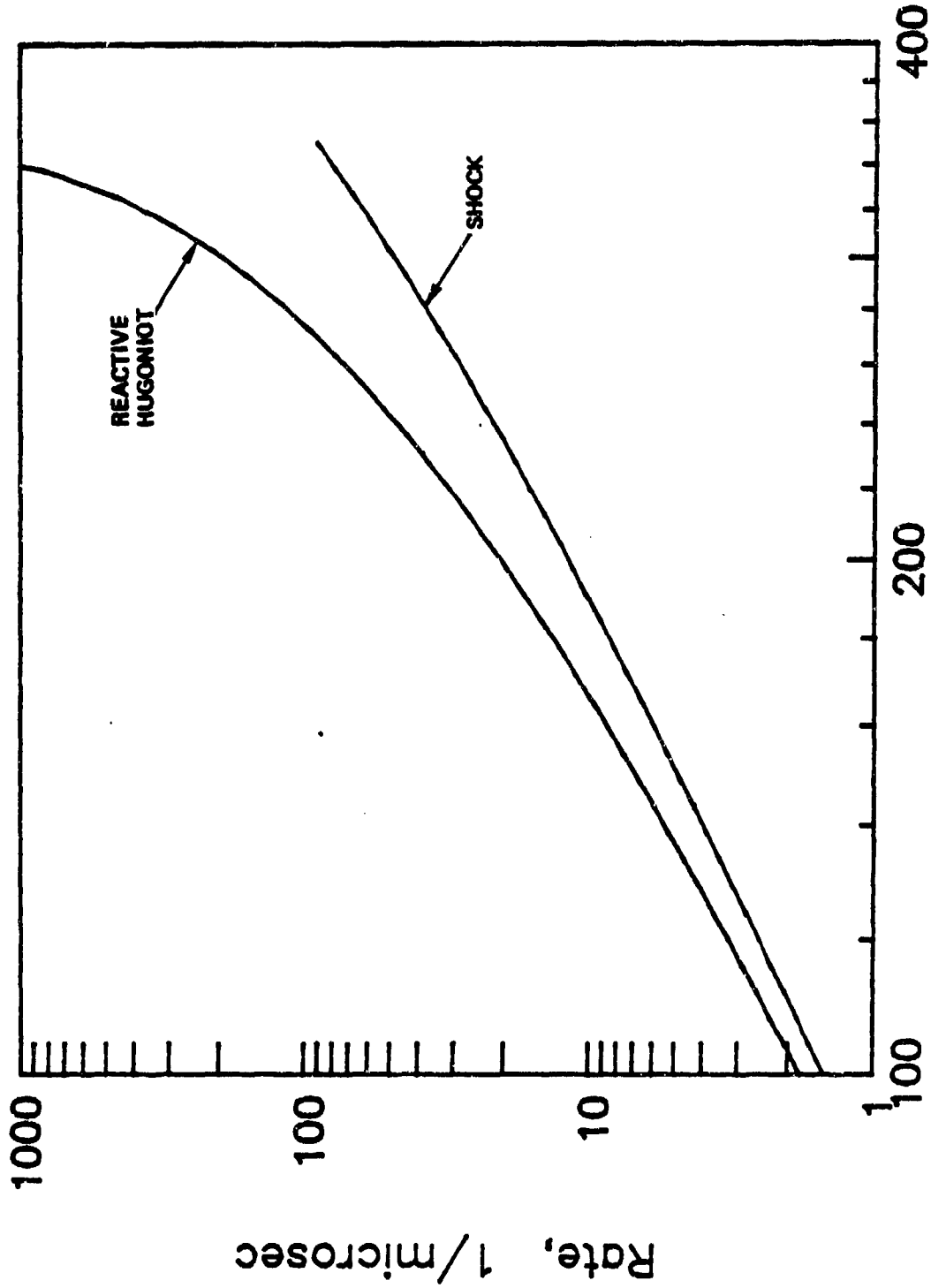

FIGURE 5. Reaction Rate – W_r/W_1 Showing Effect of First-Order Kinetics Assumption.

material. Calculations show that the run distance in the explosive depends on the shock impedance of the attenuators. To evaluate the magnitude of this effect, Figure 6 shows run distance calculated as a function of initial shock pressure for two extreme cases. In the first case, the shock was produced by the impact of a plexiglas flyer plate. In the second, the shock was generated by imposing a constant velocity (a piston) upon the boundary of the explosive material, thus simulating an infinite shock impedance. The HOM equation of state for plexiglass (Reference 2) was used. For this calculation, constant rate kinetics (Equation 21) was used for the burn model and was fitted using the nonreacting shock Hugoniot. The run distance for the plexiglass flyer plate in Figure 6 is approximately 20% longer than the corresponding distance calculated for the constant velocity piston. In the following calculations, the plexiglass flyer is used.

The influence of the reaction model on run distance is shown in Figure 7. The run distance normalized by the experimental value obtained from the Pop plot is plotted against the input shock pressure. Each of the two kinetics models is fitted to the extreme choices of nonreacting shock Hugoniots and the reacting Hugoniot which passes through the CJ point. The curves are labeled in the figure for first-order kinetics:

FF1–reacting Hugoniot
FF2–nonreacting shock

and for constant rate kinetics:

FF3–reacting Hugoniot
FF4–nonreacting shock

For the first-order kinetics model, a wide range of response can be obtained by the choice of the reacting Hugoniot. The calculated results at low initial shock pressure, however, are not very sensitive to the kinetic model or its calibration. This is because the solid mass fraction is nearly unity at low pressures on the reacting Hugoniot used for the calibration, and this condition is obtained for most of the run distance.

The difference in behavior of the different models is most extreme at the high-pressure end. This pressure region is of importance in physical problems where the detonation reaction zone must be resolved. These problems include, for example, critical diameter, response to thin, high-speed flyer plates, and minimum priming charge tests. Any calculation of these types of problems using a variation of the Forest Fire burn model should be viewed skeptically until thorough experimental verification is obtained.

One consequence of the constant rate kinetics model is that its implementation is more automatic than the first-order kinetics model. The range of calculated run distance shown in Figure 7 is much less between the reacting and nonreacting choices of Hugoniot. This means that one can get a good correlation with the wedge test experiment with a minimum of guessing at reacting Hugoniots. In this regard, however, it can be noted from Figure 7 that the constant rate curves, FF3 and FF4, are reasonably straight lines, so some improvement could be obtained by artificially modifying the input Pop plot.

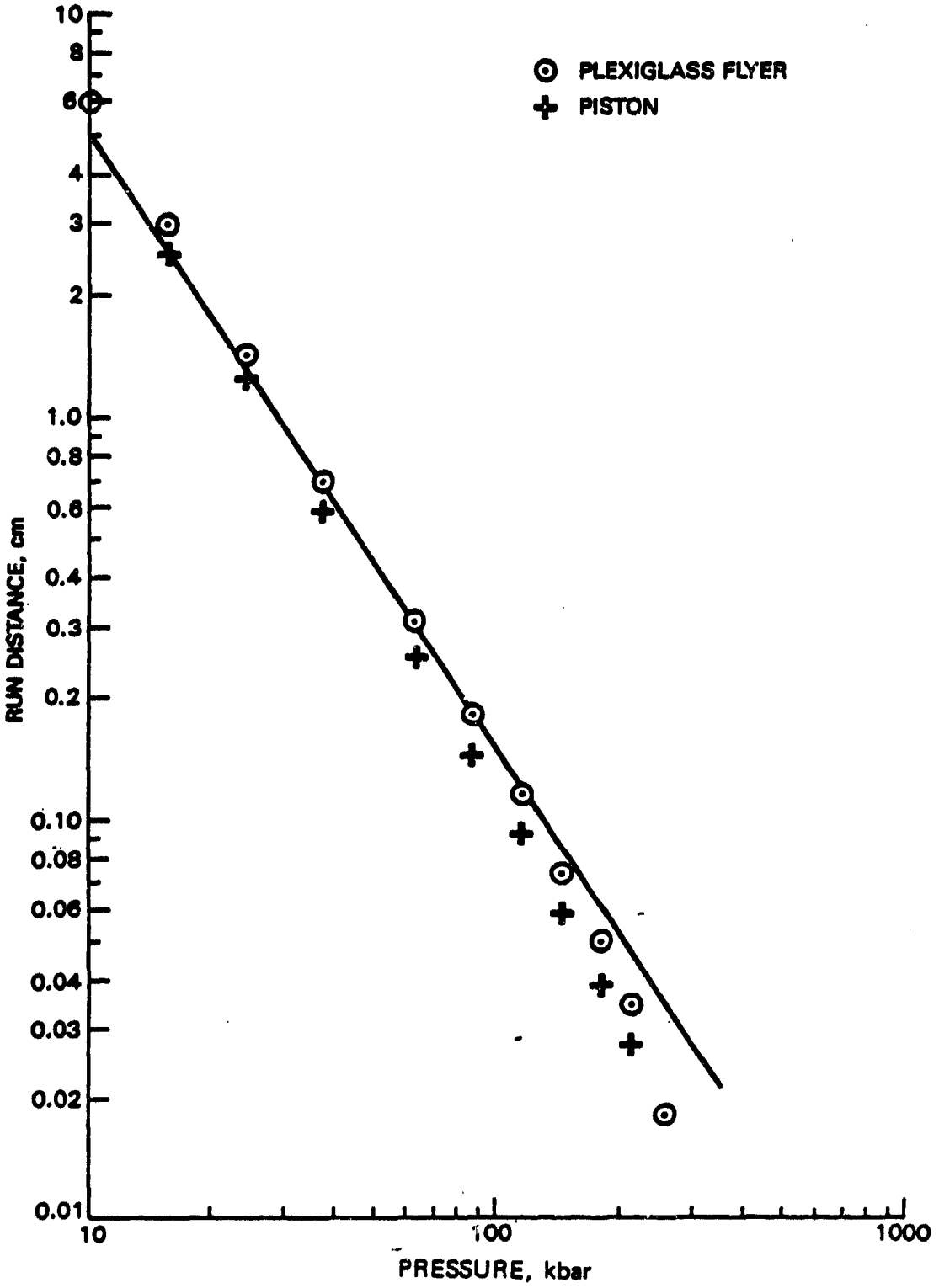

FIGURE 6 Wedge Test Simulation Showing Effect of Flyer Plate Impedance.

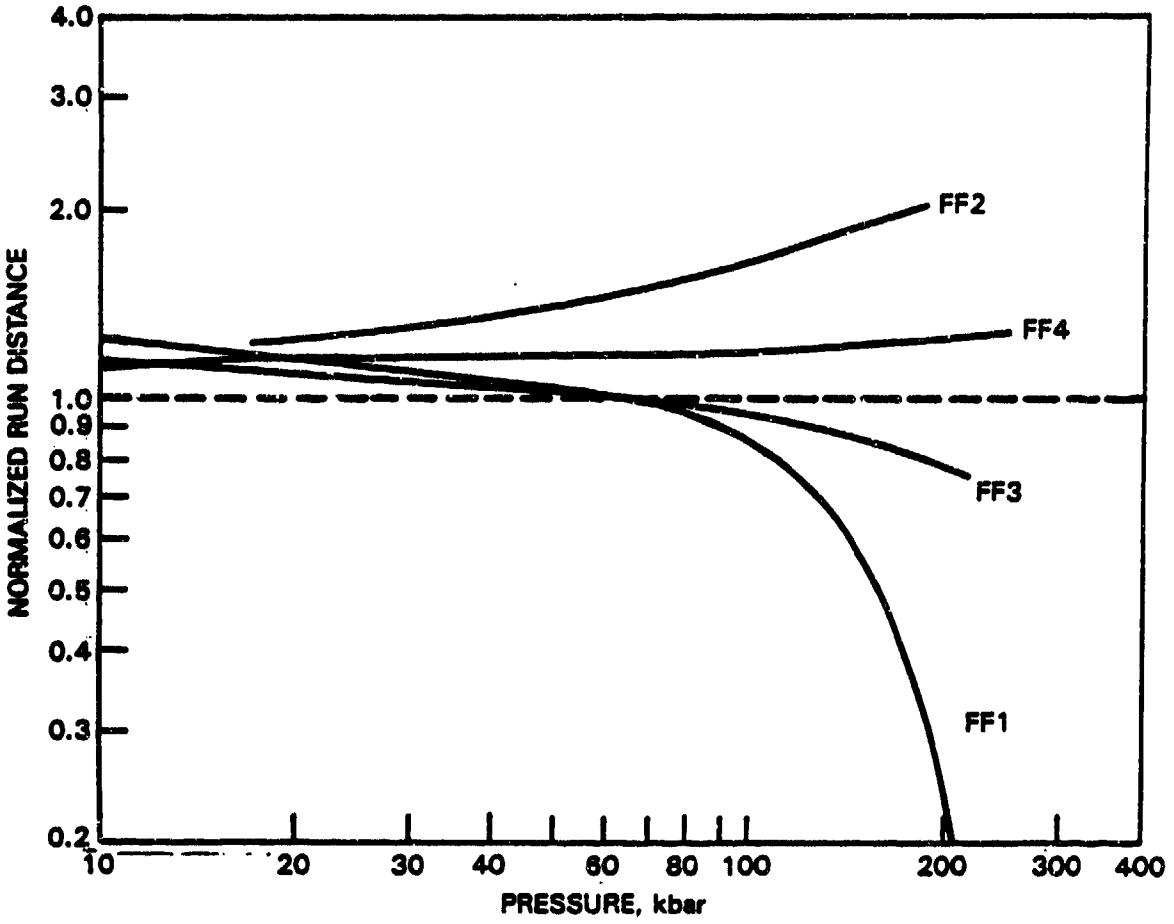

FIGURE 7. Effect of Reactive Hugoniot Assumption and Reaction Kinetics Model on Wedge Test Simulated by a Plexiglas Flyer Plate.

In the course of making the calculations, plots of pressure profiles of the reactive flow were made. Initially the pressure gradient was quite small and $P_m = 0$ appeared to be a valid assumption. However, at later times, after a period of shock acceleration, a very strong gradient developed. This being the case, it is not clear why the Forest Fire burn model gives such good overall agreement for the wedge test run distance. If one examines individual experimental wave trajectories corresponding to different initial shock pressure to verify the single-curve buildup principle, one finds curves of wave velocity, U_s, plotted against wave position, X_1, which all lie in a narrow band. However, individual shock-wave accelerations within this band can deviate substantially from the mean and from one another. One can speculate that input of an average shock trajectory will yield a good prediction of global results like run distance, even though details of the process may be erroneous.

CONCLUSIONS

The reaction rate, W_r, expressed as a function of pressure, is not sensitive to the choice of reactive or nonreactive Hugoniot used in its calibration. The choice becomes important when the formula for first-order kinetics is assumed to express the rate. With the first-order kinetics formula calibrated first using the extreme reactive and then the nonreactive Hugoniot, the calculated wedge test results bracket the experimental results. One can therefore fine-tune the agreement with experiment by adjusting the choice of reactive Hugoniot. The drawback to this approach is that neither the first-order kinetics nor the reactive Hugoniot has any physical relation to shock-initiated burning in heterogeneous explosive. A simpler constant reaction rate approach is suggested that avoids the difficulties of choosing an unphysical reactive Hugoniot while giving a satisfactory correlation with the wedge test results.

Calculations of wedge test results at low initial shock pressure were basically insensitive to the kinetic model and the Hugoniot used in its calibration. The differences were quite large, however, for wedge test calculations starting with high initial shock pressures. The reason is that at low pressure, the solid mass fraction is nearly one for most of the run distance. Under this circumstance, there is no essential difference between the various reaction models and their calibration.

The Forest Fire burn law as formulated by Forest is not applicable to high-pressure phenomena where the pressure may exceed the CJ value. This situation is obtained, for example, whenever the reaction zone in a detonation must be resolved. The constant rate approach discussed here may be a reasonable way to extrapolate moderate pressure reaction rates to pressures greater than the CJ value. The validity of this approach needs to be tested.

REFERENCES

1. Los Alamos Scientific Laboratory. "Two-Dimensional Homogeneous and Heterogeneous Detonation Wave Propagation," by C. L. Mader and C. A. Forest. Los Alamos, N. Mex., LASL, June 1976. (LA-6259, publication UNCLASSIFIED.)

2. Charles L. Mader. *Numerical Modeling of Detonations*. Berkeley and Los Angeles, University of California Press, 1979.

3. A. L. Bowman, C. A. Forest, J. D. Kershner, C. L. Mader, and G. H. Pimbley. "Numerical Modeling of Shock Sensitivity Experiments," *Proceedings of the Seventh Symposium (International) on Detonation, June 1981*. (NSWC MP-82-334, publication UNCLASSIFIED.)

4. U.S. Army Ballistic Research Laboratories. "Numerical Modeling of Projectile Impact Shock Initiation of Bare and Covered Composition B," by J. Starkenberg, Y. Huang, and A. Arbuckle. Aberdeen Proving Ground, Md., BRL, August 1984. (ARBRL-TR-02576, publication UNCLASSIFIED.)

5. C. A. Forest. "Burning and Detonation," *Proceedings of the Seventh Symposium (International) on Detonation, June 1981*. (NSWC MP-82-334, publication UNCLASSIFIED.)

6. J. J. Dick. "Buildup to Detonation in Solid High Explosives During Plane Shock Initiation: Some Comparisons," *Proceedings of the Eighteenth Symposium (International) on Combustion, 1981*.

7. *Los Alamos Scientific Laboratory*. "HYDROX, A One-Dimensional Lagrangian Hydrodynamics Code," by M. S. Shaw and G. K. Straub. Los Alamos, N. Mex., LASL, March 1981. (LA-8642-M, publication UNCLASSIFIED.)

8. V. N. Kondrat'ev. *Chemical Kinetics of Gas Reactions*. New York, Pergamon Press, 1964.

9. E. L. Lee and C. M. Tarver. "Phenomenological Model of Shock Initiation in Heterogeneous Explosives," *Phys. Fluids*, Vol. 23 (1980), p. 2362.

10. C. M. Tarver and J. O. Hallquist. "Modeling Two-Dimensional Shock Initiation and Detonation Wave Phenomena in PBX 9404 and LX-17," *Proceedings of the Seventh Symposium (International) on Detonation, June 1981*. (NSWC MP-82-334, publication UNCLASSIFIED.)

11. T. R. Gibbs and A. Popolato. *LASL Explosive Property Data*. Berkeley and Los Angeles, University of California Press, 1980.

INITIAL DISTRIBUTION

9 Naval Air Systems Command
  AIR-5004 (2)
  AIR-540 (2)
  AIR-93 (2)
  AIR-932D (1)
  AIR-932J, B. Warren (1)
  AIR-932K (1)
6 Chief of Naval Operations
  OP-03 (2)
  OP-05 (1)
  OP-098 (1)
  OP-354 (1)
  OP-55 (1)
2 Chief of Naval Research, Arlington
  OCNR-10P (1)
  OCNR-1131 (1)
11 Naval Sea Systems Command
  SEA-09B312 (2)
  SEA-62D (5)
  SEA-62E (2)
  SEA-662 (2)
1 Commander in Chief, U. S. Pacific Fleet (Code 325)
1 Air Test and Evaluation Squadron 5, China Lake
1 Commander, Third Fleet, Pearl Harbor
1 Commander, Seventh Fleet, San Francisco
1 David Taylor Naval Research Center, Bethesda
2 Naval Academy, Annapolis (Director of Research)
1 Naval Air Force, Atlantic Fleet
2 Naval Air Force, Pacific Fleet
1 Naval Air Station, North Island
2 Naval Air Test Center, Patuxent River (Central Library)
1 Naval Avionics Center, Indianapolis (Technical Library)
1 Naval Explosive Ordnance Disposal Technology Center, Indian Head
1 Naval Ocean Systems Center, San Diego (Code 447)
1 Naval Ordnance Station, Indian Head (Technical Library)
1 Naval Postgraduate School, Monterey (Technical Library, G. Kinney)
1 Naval Research Laboratory (A. Williams)
4 Naval Surface Warfare Center, Dahlgren
  G13
    D. Dickinson (1)
    T. Wasmund (1)
  G22, W. Holt (1)
  G25, T. Swiark (1)
10 Naval Surface Warfare Center, White Oak Laboratory, Silver Spring
  R10
    H. Haiss (1)
    S. Jacobs (1)
  R10E, J. Kelley (1)
  R12, J. Erkman (1)
  R13
    K. Kim (1)
    R. Liddiard (1)
    J. Short (1)
    M. Swisdak (1)
  Guided Missile Warhead Section (1)
  Technical Library (1)

1 Naval War College, Newport
1 Office of Naval Research Detachment (Pasadena), Pasadena
1 Office of Naval Technology, Arlington (OCNR-20)
1 Operational Test and Evaluation Force, Atlantic
2 Pacific Missile Test Center, Point Mugu
  Code 1245, Nofrey (1)
  Technical Library (1)
1 Marine Corps Air Station, Beaufort
1 Army Armament Munitions and Chemical Command, Rock Island (DRSAR-LEP-L, Technical Library)
3 Army Missile Command, Redstone Arsenal
  AMSMI-RD-PR-M (1)
  AMSMI-RD-PR-S (1)
  DASD-H-SST, J. Rutland (1)
1 Aberdeen Proving Ground (Development and Proof Services)
13 Army Ballistic Research Laboratory, Aberdeen Proving Ground
  AMSAA
    C. Alston (1)
    Bloemquist (1)
  AMXAR-SKI-B (1)
  AMXAR-T, Detonation Branch (1)
  AMXAR-TSB-S (STINFO) (1)
  AMXBR-TBD
    J. Dahn (1)
    J. Kenecke (1)
  AMXBR-VLDA, T. Bentley (1)
  AMXY-AD (1)
  AMXSY-J (1)
  DRDAR-BLT
    R. Frey (1)
    P. Howe (1)
    J. Starkenberg (1)
1 Army Materiel Systems Analysis Activity, Aberdeen Proving Ground (K. Meyers)
2 Army Research Office, Research Triangle Park
  DRXRO-IP-L, Information Processing Office (1)
  Dr. E. Saible (1)
1 Harry Diamond Laboratories, Adelphi (Technical Library)
1 Radford Army Ammunition Plant
2 Rock Island Arsenal
  Navy Liaison Office (NVLNO) (1)
  Technical Library (SARRI-ADM-P) (1)
1 White Sands Missile Range (STEWS-AD-L)
1 Yuma Proving Grounds (STEYT-GTK, M&W Branch)
4 Air Force Armament Division, Eglin Air Force Base
  AFATL/DLJW, J. Foster (1)
  AFATL/DLODL, Technical Library (1)
  AFATL/DLYV
    G. Crews (1)
    K. McArdle (1)
1 Air Force Intelligence Service, Bolling Air Force Base (AFIS/INTAW, Maj. R. Lecklider)
1 Air University Library, Maxwell Air Force Base
1 Tactical Fighter Weapons Center, Nellis Air Force Base (CC/CV)
2 57th Fighter Weapons Wing, Nellis Air Force Base
2 554th Combat Support Group, Nellis Air Force Base
  OT, FWW/DTK (1)
  OT, FWW/DTO (1)
1 Defense Advanced Research Projects Agency, Arlington (Materials Science Division, Snow)
1 Defense Nuclear Agency (Shock Physics Directorate)
12 Defense Technical Information Center, Alexandria
1 Department of Defense-Institute for Defense Analyses Management Office (DIMO), Alexandria
1 Lewis Research Center (NASA), Cleveland
1 Aerojet Liquid Rocket Company, Sacramento, CA (Library)

3 Applied Ordnance Technology, Arlington, CA
  R. Beauregard (1)
  H. Benefiel (1)
  E. Daugherty (1)
1 Atlantic Research Corporation, Gainesville, VA (K. Graham)
2 Colorado Seminary, Denver Research Institute, Denver, CO
  R. Recht (1)
  J. Yatteau (1)
2 Comarco, Ridgecrest, CA
  M. E. Backman (1)
  R. G. S. Sewell (1)
1 California Institute of Technology, Jet Propulsion Laboratory, Pasadena, CA (Technical Library)
2 Hercules, Incorporated, Allegany Ballistics Laboratory, Rocket Center, WV (Library)
1 Hercules, Incorporated, Bacchus Works, Magna, UT (Library)
1 IIT Research Institute, Chicago, IL (Department M, Document Librarian)
4 Los Alamos National Laboratory, Los Alamos, NM
  A. Bowman (1)
  C. Forest (1)
  R. Rabie (1)
  Reports Library (1)
1 Morton-Thiokol Corporation, Brigham City, UT (via AFPRO) (D. Clark)
1 Morton-Thiokol Corporation, Elkton, MD (Library)
1 Morton-Thiokol Corporation, Huntsville, AL (W. B. Thomas)
3 New Mexico Institute of Technology, Center for Explosive Technology Research, Socorro, NM
  B. Craig (1)
  T. Joyner (1)
  P. Persson (1)
1 Princeton University, Forrestal Campus Library, Princeton, NJ
1 Stanford Research Institute, Poulter Laboratories, Menlo Park, CA
1 The Boeing Company, Seattle, WA (E. Wilhelm)
2 The Johns Hopkins University, Applied Physics Laboratory, Laurel, MD (Document Library)
2 The Johns Hopkins University, Applied Physics Laboratory, Chemical Propulsion Information Agency, Laurel, MD
1 The Rand Corporation, Santa Monica, CA (Technical Library)
1 United Technologies Corporation, Chemical Systems Division, San Jose, CA (Library)
5 University of California, Lawrence Livermore National Laboratory, Livermore, CA
  L324, M. Finger (1)
  L39, Landingham (1)
  E. Lee (1)
  Reports Library (1)
  C. Tarver (1)

ON CENTER DISTRIBUTION

1 Code 01
1 Code 12
1 Code 31
1 Code 32
1 Code 3205I, A. Victor
2 Code 3267
  R. Hoffman (1)
  Lind (1)
1 Code 33
1 Code 33505, P. Yates
4 Code 343 (3 plus Archives copy)
2 Code 3686, GIDEP
1 Code 38
2 Code 389
2 Code 3891
  M. Chan (1)
  H. Richter (1)
25 Code 3894
  M. Alexander (1)
  O. Heimdahl (1)
  E. Lundstrom (21)
  J. Schulz (1)
  M. Wagenhals (1)
1 Code 39
1 Code 62
1 Code 6203